STUDY OF THE SIO_2 PLASMA RADIATION. APPLICATION TO THE FUSE ARC PLASMA

William Bussière[1], David Rochette[2], Pascal André[1], Gérard Velleaud[2] and Steeve Memiaghe[1]

[1] LAEPT CNRS UMR 6069, Phys. Bât. 5, Université Blaise Pascal, 24 Avenue des Landais, F63177 AUBIERE Cedex, France, Phone: +33 4 73 40 77 04, Fax: +33 4 73 40 76 50, william.bussiere@univ-bpclermont.fr, steeve.memiaghe@univ-bpclermont.fr, pascal.andre@univ-bpclermont.fr

[2] LAEPT CNRS UMR 6069, Université Blaise Pascal, IUT de Montluçon, Avenue Aristide Briand, BP 2235, F03101 Montluçon Cedex, France, Phone: +33 4 70 02 20 16, Fax: +33 4 70 02 20 78, rochette@moniut.univ-bpclermont.fr, gerard.velleaud@moniut.univ-bpclermont.fr

Abstract: **During the HBC fuse working, the fault current implies the initiation of an electric arc which is composed of metallic species vapours mainly, generally silver. This defines the end of the pre-arcing time. This electric arc interacts quickly with the surrounding silica sand grains or quartz sand. Thus a silver plasma is formed around the reduced sections of the fuse element. This silver plasma interacts with the silica sand grains and this interaction gives rise to the ignition of a plasma composed of vapours resulting from the dissociation of the SiO_2 molecules. The radiation escaped from the SiO_2 plasma can be used to assess experimentally the temperature (T) and the electron density (n_e), two fundamental parameters for modelling purposes. T and n_e are difficult to interpret because of the strong gradients in pressure, temperature, and material densities from the centre to the surroundings where the measurement is done. We propose a first formulation to calculate this radiation in order to increase the understanding of the radiation measurements.**

Keywords: **SiO_2 plasma, fuse arc plasma, radiation, continuum, discrete radiation.**

1. Introduction

This paper is especially concerned by HBC fuse that basically comprises: two electrodes, the fuse element (generally in silver), the filling cavity, and the arc quenching material that is to say the silica sand (or quartz sand). The aim of the study is to give a first assessment by calculation to the radiative properties of the fuse arc plasma initiated during the fuse working. In fact many attempts have been done in the past to evaluate the temperature [1-4] and the electron density [5-8] by means of the study of the discret radiation emitted either by the metallic species or the silicon lines observed in the neutral state, or ionised once or twice. From the set of papers published until now several disparities are observed in the temperature and electron density results.

This work is especially focussed on the understanding of the spectral line shapes of the silicon lines ionised once. In many studies the temperature is obtained from the classical method by calculating the ratio of the intensities of these Si II lines. This method implies to consider a Boltzmann law for the energy level distribution, and to assume that the Local Thermodynamic Equilibrium (LTE) is valid. These hypotheses are discussed in Section 4. The Si II lines are also used to assess to the electron density [1, 5, 6, 9]. In this case the Stark broadening is assumed to be the greatest broadening for the considered spectral lines.

Many studies have depicted the burn-back – erosion of the fuse element – and the evolution of the fulgurite volume during the fuse working [10-12]. It is well known that the SiO_2 plasma is defined by a strong temperature – about 20,000 K at the most [5, 6, 9] – a high electron density – about 10^{18} cm^{-3} to 10^{19} cm^{-3} at the most [1,9] – and a strong pressure – about 10 to 50 bars [13, 14]. This plasma is surrounded by a concentric layer made of fused silica with partly eroded sand gains inside. And this layer is itself surrounded by solid silica sand grains. So there exist very strong gradients in temperature, density and pressure from the centre to the point of observation, which are responsible for more or less absorption of the radiation escaped from the core of the SiO_2 plasma. At our knowledge there is no published study concerning the calculation of the radiation for Ag_SiO_2 plasma, except in [15]. But in this latter study the intensity of the monoatomic spectral lines is calculated without taking into account the influence of the broadening mechanisms on the resulting spectral line shape and thus on the intensity of the radiations. To obtain such results it is necessary to calculate the volumetric emission coefficient, and thus to depict the broadening mechanisms.

 978-2-84516-363-8/07/$25.00 © 2007
Blaise Pascal Academic Press

In Section 2 we depict briefly the observation of the radiation with our experimental fuse and the assessment of the temperature. In Section 3 we give the formulation used to calculate the radiation emitted by a SiO_2 plasma by distinguishing the continuum and the discrete line emission. The calculated results are given for the SiO_2 plasma by considering various configurations for the gradients.

2. Light emission during the fuse working

2.1. Industrial fuse and experimental fuse

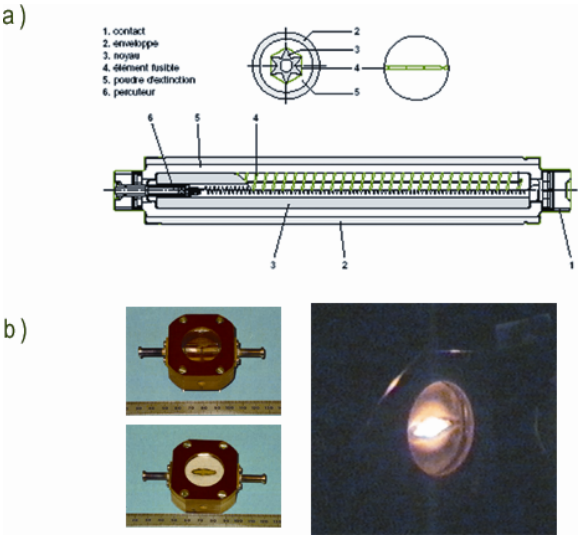

Fig. 1: a) Schematic view of a typical industrial fuse [16]. b) Experimental fuse designed to spectroscopic observations (before the test, during the test with a strong radiation, and after the test with the fulgurite) [9].

The observation of the light escaped from the fuse arc plasma is impossible in the case of an industrial fuse because of the closed filling cavity (Fig.1.a). In the case of an experimental fuse (Fig.1.b) a quartz window can be fitted on the fuse cartridge to collect directly the radiation [9] ; or instead of a quartz window, an optical fibre can be inserted directly through the silica sand, the light being collected by the optical fibre end close to the plasma volume [4, 5, 6]. In this latter case the optical fibre end can be damaged due to the plasma proximity because of the very high temperature. So the properties – optical and geometrical – of the collecting end change during the measurement. And the interpretation of the measurement is difficult.

In the case of the quartz window the hot plasma interacts with the window during the fuse working. This implies the shift of the plasma volume on the quartz area. This shift can be limited if the section of the fuse element is directly put on the quartz window, rather than putting the fuse ribbon over the plane defined by the window. The escaped radiation is focussed by means of a lens to the entrance end of an optical fibre connected to the entrance slit of a Chromex spectroscope equipped with a 1,242×1,152 CCD matrix [8]. The use of this CCD matrix in kinetic mode allows the assessment of the evolution of the temperature on the whole duration of the fuse working.

Therefore the light escaped from the centre of the radiating plasma volume is integrated over a depth that is not known with an outer limit defined by the quartz window. This depth can be estimated around the initial width of the fuse strip. Over this depth the collected radiation crosses many layers with different values for the temperature, the pressure and the density.

2.2. Measurement of the temperature

The evolution of the temperature on the fuse working duration is obtained by studying the Si II (1) and (3) triplets radiation [9] and taking into account the calculated intensity ratios according to LS coupling for the energy levels within a multiplet [17]. Considering the Boltzmann law for the energy levels at a given temperature, the total intensity of a spectral line $I_{SiII,ul}$ of frequency ν_{ul} is given by:

$$I_{SiII,ul} = \frac{1}{4\pi} \cdot \frac{h\nu_{ul}}{c} \cdot L \cdot g_u \cdot A_{ul} \cdot \frac{N(T)}{U(T)} \cdot e^{-\frac{E_u - E_l}{kT}} \quad (1)$$

where: g_u is the statistical weight of the upper emitting level u, A_{ul} is the transition probability from the upper level u to the lower level l, L is the optical thickness of the radiating volume, $N(T)$ is the total density of the radiating species Si II, $U(T)$ is the Si II internal partition function, E_u and E_l are respectively the upper and lower energy levels of the studied radiation, and T is the temperature identified to the excitation temperature. If we consider two lines from Si II (1) and Si II (3), the temperature T can be obtained without the calculation of $N(T)$ and $Z(T)$.

From Eq.(1) we notice that the temperature assessment is sensitive to four main factors.

The uncertainty for the A_{kj} values

For the two stronger lines of Si II (1), 385.602 nm and 386.260 nm, the estimated accuracy is inferior to 18%, and for the two stronger lines of Si II (3), 412.807 nm and 413.089 nm, the estimated accuracy is inferior to 10% [18].

The optical thickness L

It depends in part of the wavelengths of the studied spectral lines. In our case the triplets Si II

978-2-84516-363-8/07/$25.00 © 2007
Blaise Pascal Academic Press

(1) and (3) are separated by about 27 nm, which can be considered as weak in regards to the other factors influencing the measurement of the temperature.

The calibration in intensity of the CCD matrix

An absolute calibration in intensity is necessary if the temperature is deduced from the absolute intensity of the spectral lines. In this case one temperature is deduced from each studied line. The use of this method is difficult in our case because of the various possible errors linked to the optical device and the fluctuations of the radiating volume. But a calibration is necessary to calibrate the response of the optical line and of the spectroscope plus CCD matrix. This is done by using a calibrated tungsten ribbon lamp [8]. Thus the experimental acquisition is corrected for the given spectral interval comprises the four Si II lines.

The experimental assessment of the intensity $I_{SiII,jk}$ *of the studied line*

Usually a direct assessment of the total area of the spectral lines is good enough. In the case of the fuse arc plasma, and because of the strong values for the electron density and the pressure, it is necessary to fit the experimental spectral line profile by using a profile taking into consideration the physical effects responsible for the broadening of the observed lines. In our case the experimental profiles are fitted by means of a Voigt profile [8]. This profile results from the combination of a Gaussian profile: apparatus function, Doppler broadening, and of a Lorentz profile: natural, Van der Waals, resonance and quadratic Stark broadenings.

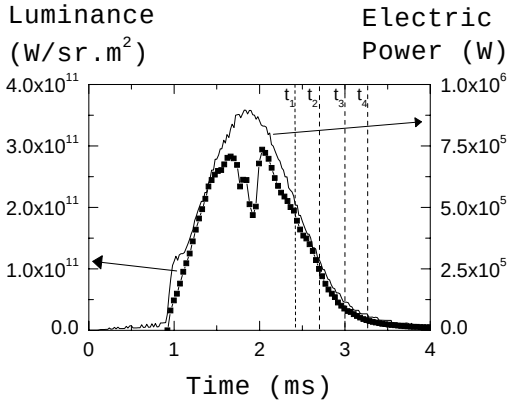

Fig. 2: Evolution versus time of the total intensity or luminance observed in the range 360 nm-800 nm and of the electric power [8]. Fuse test performed with a capacitor bank discharge (stored voltage: 460 V, presumed current: 3.2 kA, pre-arcing time: 0.9 ms). The times t_1, t_2, t_3 and t_4 correspond to the calculation of the radiation (Section 3.2)

2.3. Light emission during the fuse working

The intensity of the total radiation escaped from the fuse arc plasma is directly linked to the instantaneous electric power. The evolution versus time of the luminance and of the electric power is given in Fig. 2. The radiation is integrated for the spectral interval [360-800] nm. At the beginning of the arcing time the luminance increases as the electric power (from 0.9 ms to ~1.5 ms). Due to the energy brought by the fault current the energy of the plasma increases. The losses of energy linked to the cooling of the plasma increases, especially the radiation. The opposite trend is observed at the decrease of the current (from ~2.1 ms to 4 ms). There exists a particular decrease in luminance for the time scale corresponding to the higher values of the electric power. Moreover the higher values in pressure are also observed for this time scale.

From the Figure 2 the influence of the radiation absorption appears clearly. As the temperature and the electron density are deduced from the study of the radiation properties, it is necessary to understand what could be the influence of the density, the pressure on the escaped radiation. In fact these latter parameters are directly linked to the density and the temperature of the radiating species, to the absorption of the escaped radiation when it crosses various layers in the plasma volume from the hot centre to the colder surroundings.

3. Calculation of the radiation

The radiation intensity is expressed in terms of the spectral emission coefficient (ε_λ) which is the result of [19-23]:

3.1. Spectral line

Spectral emissivity for one isolated line

For each radiating species one defines the spectral emissivity by [19]:

$$\varepsilon_{i,ul,\lambda}(\lambda,T)=\frac{h.c}{4\pi}\times A_{i,ul}\times n_{i,u}(T)\times P_{i,ul}(\lambda,T) \qquad (2)$$

where $A_{i,ul}$ is the transition probability from the upper energy level u to the lower energy level l, $n_{i,u}(T)$ is the population density for the energy level E_u corresponding to the ith radiating species at temperature T, $P_{i,ul}(\lambda,T)$ is the normalized spectral profile at temperature T. For the spectral lines studied in this work the transition probabilities are obtained from [18]. The population density $n_{i,u}(T)$ for the ith species is deduced from:

978-2-84516-363-8/07/$25.00 © 2007
Blaise Pascal Academic Press

$$n_{i,u}(T) = \frac{n_i(T) g_u}{Z(T)} \times e^{-\frac{E_u}{kT}} \times \omega_u \quad (3)$$

where $n_i(T)$ is the total density of the i[th] species at temperature T, g_u is the statistical weight for the upper energy level E_u, $Z(t)$ is the total partition function [15,37-38], and ω_u is the population probability of the corresponding energy level [18]. In the case of the fuse arc plasma the use of an approximate profile $P_{i,ul}(\lambda,T)$ is enough especially as the use of a precise Voigt profile is computationally expensive. The normalized spectral profile $P_{i,ul}(\lambda,T)$ is evaluated by using the approximate formula [19]:

$$P_{i,ul}(\lambda,T) = \frac{\varepsilon_{i,L_{ul},\lambda_{ul}}}{\varepsilon_{i,L_{ul},\text{int}}} \times f_{i,w_L,w_V,\lambda_{ul}}(\lambda) \quad (4)$$

where $f_{i,w_L,w_V,\lambda_{ul}}(\lambda)$ is a numerical expression defined for the studied line of wavelength λ_{ul}, w_L is the Lorentz half-width, w_V is the Voigt half-width. The two terms $\varepsilon_{i,L_{ul},\lambda_{ul}}$ and $\varepsilon_{i,L_{ul},\text{int}}$ are respectively the centreline magnitude and the integrated intensity for the studied line [19]. The following items consist in a depiction of the physical broadening mechanisms responsible for the Lorentz and Gaussian half-widths [22].

Broadening mechanisms resulting in a Gaussian profile

• The Doppler broadening is described by a Gaussian profile and is of negligible contribution in the total half-width.

• The apparatus function is not generated by a physical mechanism. It is the response of the monochromator plus CCD matrix device to an isolated and thin line. It has to be taken into account especially at the end of the arcing period because the spectral lines are weakly broadened.

Broadening mechanisms resulting in a Lorentz profile

• The resonance broadening is due to an atom or ion in a resonance state interacting with another like atom of ion in a ground state. It is not the case for the once ionised silicon lines studied.

• The natural broadening is due to the finite lifetimes of an atom or ion. It is calculated using the formulation given in [22] but it is of negligible contribution for the studied lines.

• The Van der Waals broadening is of great contribution in the case of neutral emitters. In the case of the once ionised silicon lines, this broadening exists but it is negligible. An approximated calculation can be made with the hydrogenic assumption [19].

• The Stark broadening is the greatest contribution in the case of the studied plasma. In fact the fast energy release linked to the power supply produces silica vapours from the early beginning of the arcing period. These vapours are enclosed in a surrounding fused silica layer which maintains an overpressure on the plasma volume. Because of the energy of the fault current the temperature of the plasma increases, and so does the amount of vapours. Thus the pressure of the plasma increases strongly [13-14]. Therefore the number and the strength of the collisions between charged particles increase which imply the splitting of the emitting energy levels of the radiating atom or ion. In the case of a plasma the quadratic Stark broadening is dominant in comparison to the linear Stark broadening, and it can be evaluated using the results given by Griem [24-25].

Resulting Voigt profile

The resulting profile is known as the Voigt profile, with the half-width defined by [19]:

$$w_V = \frac{w_L}{2} + \sqrt{\frac{w_L^2}{2} + w_G^2} \quad (5)$$

where w_G and w_L are respectively the Gaussian half-width and the Lorentzian half-width taking into account each of the broadening mechanisms defined.

3.2. Continuous radiation

There exist many works dedicated to the calculation of the continuous radiation [26] in the case of the most common elements such as H_2, He, N_2, O_2 [27], Ar [28], SF_6 [29], rare gases [30] [31] [32] and highly ionised elements. Some information can also be found about the calculation of the volumetric emission coefficient dedicated to typical applications such high current breakers [33-34].

For the calculation of the continuum, two contributions are calculated, namely the free-bound continuum and the free-free continuum. Considering that the aim of the study is a first step in the understanding of the radiated properties in electric fuses on one side, and that the fuse plasma is characterized by strong values of the temperature, electron density and pressure on the other side, the molecular contribution is neglected. This latter assumption supposes that the chemical species in the plasma are completely dissociated.

Free-bound continuum

The free-bound continuum or recombination radiation is due to the capture of a free electron by an ion. The contribution of the continuum due to negative ions (attachment of an electron to an atom or a molecule) is neglected is so far as the concentration of these negative ions is very low

978-2-84516-363-8/07/$25.00 © 2007
Blaise Pascal Academic Press

compared to the other contributing species [15]. The free-bound continuum is defined from the ξ_{fb} factor or Biberman factor [19] by:

$$\varepsilon_{fb,\lambda,i,z\geq 2} = 2.177\times\frac{e^6}{c^2 m_e^{1.5}}\sqrt{\frac{\pi}{k}}\frac{g_{i,z,1}}{U_{i,z}} \times\frac{n_e n_{i,z}(z-1)^2}{\lambda^2\sqrt{T}}\times\left(1-e^{-\frac{hc}{\lambda kT}}\right)\times\xi_{fb,i,z}(T,\lambda) \quad (6)$$

where e is the elementary charge, c is the speed of light, m_e is the electron mass, $g_{i,z,1}$ is the statistical weight of the ground state for the particle i in the ionisation stage z (z =1 for atom, z =2 for the first ion, etc.), $U_{i,z}$ is the partition function, n_e is the electron density, $n_{i,z}$ is the density of particle i in the ionisation stage z, λ is the wavelength, T is the temperature, h is the Planck constant, k is the Boltzmann constant, $\xi_{fb,i,z}$ is the Biberman factor whose values are tabulated in [35]. In this study the equation is given in absorption coefficient form.

Free-free continuum

The free-free radiation corresponds to the emission of a photon when an electron is subjected to the electric field of an ion (case 1), or an atom subjected to a transition from a free state to another free state with lower kinetic energy (case 2). In the case 1 the free-free continuum is given by:

$$\varepsilon_{ff,\lambda,i,z\geq 2} = 2.177\times\frac{e^6}{c^2 m_e^{1.5}}\sqrt{\frac{\pi}{k}} \times\frac{n_e n_{i,z}(z-1)^2}{\lambda^2\sqrt{T}}\times e^{-\frac{hc}{\lambda kT}}\times g_{ff,z\geq 2}(T,\lambda) \quad (7)$$

where the free-free Gaunt factor is used to correct the non-classical behaviour:

$$g_{ff,z\geq 2}(T,\lambda) = 1+0.1728\times\left(\frac{hc}{\lambda E_H(z-1)^2}\right)^{1/3} \times\left(1+\frac{2kT\lambda}{hc}\right) \quad (8)$$

where E_H is the ionization energy of hydrogen. The expression (8) is defined from the hydrogenic approximation [36]. In the case 2 the following equation is used to calculate the free-free continuum:

$$\varepsilon_{ff,\lambda,i,z=1} = 3.771\times\frac{e^2}{c^2}\times\left(\frac{k}{\pi m_e}\right)^{1.5}\times\frac{n_e n_{j,z}}{\lambda^2}\sqrt{T} \times Q(T)\times\left[\left(1+\frac{hc}{\lambda kT}\right)^2+1\right]\times e^{-\frac{hc}{\lambda kT}} \quad (9)$$

where $Q(T)$ is the electron-neutral collision cross-section. This term can be neglected in the case of the fuse arc plasma in so far as it is important at low temperatures.

Resulting continuum for the fuse arc plasma

The total continuum is the sum of the free-bound and free-free continuum calculated for all the chemical species observed in the fuse arc. These chemical species can be deduced from the calculation of the plasma composition published in [15, 37-38] where the chemical species concentration is given versus the temperature. For the current paper the chemical species considered are: Si, Si^+, Si^{++}, Si^{+++}, Si^-, O, O^+, O^{++}, O^{+++}, O^- and electrons. These chemical species are chosen because:

• the calculation is made in the case of spectral observations obtained for high level of the electric power;

• from measurements we know that the temperature is high;

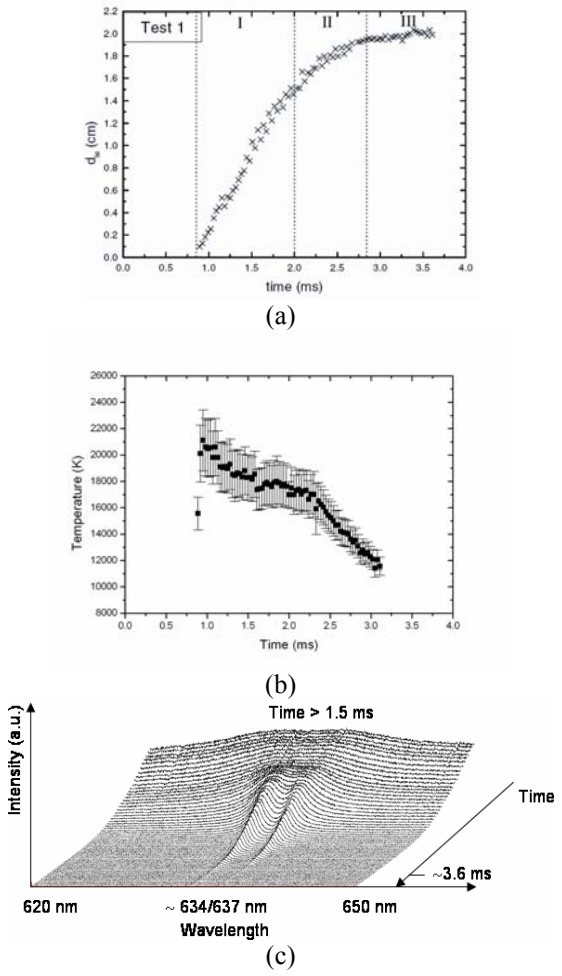

Fig. 3: Evolution versus time of: (a) length between electrodes (d_{ie}) [12], temperature [9], spectral radiation observed in the domain focussed around the Si II (2) multiplet.

978-2-84516-363-8/07/$25.00 © 2007
Blaise Pascal Academic Press

• for the time of observation, the gap between the two eroded parts of the fuse element is around 15 mm to 20 mm ; thus the silver element is supposed to be emitted in the surroundings of the plasma volume, near the two erosion fronts ; and the spectral observations are done close to the centre of the initial reduced section.

The evolution of the temperature, the inter-electrodes length, and the observed radiation in the spectral domain focussed around 634 nm is given in Fig. 3.

The radiation escaped from the fuse arc plasma is difficult to study in a spectroscopic way. This is due to the strong gradients in temperature, pressure and density from the centre to the colder surroundings. It can be easily seen in Fig. 3 (c). The quoted spectral domain comprises the Si II lines used to assess the electron density assuming that the Stark broadening is the major broadening effect [9]. The beginning of the emission starts around 0.9 ms and is not shown. We give the radiation after around 1.5 ms for which the maximum value of the electric power is observed.

The current calculation is made to understand the profile line shape observed for the Si II (2) multiplet during the decrease of the electric power, that is to say to understand the physical conditions responsible for the emission of radiation.

Resulting radiation for the fuse arc plasma

The first step is to calculate the total spectral emissivity defined by:

$$\varepsilon_\lambda(\lambda,T) = \varepsilon_{i,ul,\lambda}(\lambda,T) + \varepsilon_{fb,\lambda,i}(\lambda,T) + \varepsilon_{ff,\lambda,i}(\lambda,T) \quad (10)$$

which is expressed in $W/sr.m^4$.

To compare the experimental spectral observation with the calculated one, one had to calculate the spectral intensity in $W/sr.m^3$ defined by:

$$I_\lambda(R) = \int_0^R \varepsilon_\lambda(x,T).\exp\left(-\int_x^R k_\lambda(x',T)dx'\right).dx \quad (11)$$

where R indicates the edge of the integration domain (Fig. 4), k_λ is the spectral absorption coefficient in m^{-1} defined by:

$$k_\lambda = \frac{\lambda_{ul}^4}{8\pi c} A_{ul} g_u \frac{n_Z}{U_Z} \times \left(e^{-\frac{E_l}{kT}} - e^{-\frac{E_u}{kT}}\right).P_\lambda \quad (12)$$

The expression (12) can be used to evaluate the optical thickness $\tau_\lambda(x,T)$.

3.3. Spectral radiation for the fuse arc plasma

The calculation is done for the Si II lines of the multiplet (2) whose spectroscopic constants are given in Table 1. These lines are chosen because they are used for the electron density evaluation on one side, and they are isolated from other lines observed in the whole spectrum on the other side. Thus the pseudo-continuum due to the merging of the wings of strongly broadened lines can be neglected for the calculation.

Table 1. Spectroscopic constants for the two Si II lines of the multiplet (2) [18].

λ nm	Transition	A_{ul} 10^8 s^{-1}	g_u g_l	E_u / eV E_l / eV
634.711	$4s\ ^2S_{\frac{1}{2}} - 4p\ ^2P^0_{\frac{3}{2}}$	7.0 10^{-1}	4 2	10.073961 8.121089
637.137	$4s\ ^2S_{\frac{1}{2}} - 4p\ ^2P^0_{\frac{1}{2}}$	6.9 10^{-1}	2 2	10.066524 8.121089

The calculation is made for two times of observation during the fuse working. In this case the prospective current is provided by a capacitor bank discharge with $\hat{I}_p \sim 3.2$ kA, $V_{\sup ply} \sim 460$ V [8]. The pre-arcing time is around 0.87 ms and the arcing time is around 3 ms. The fuse element put in the tests is equipped with two reduced sections, 5 mm in width, 0.105 mm in thickness.

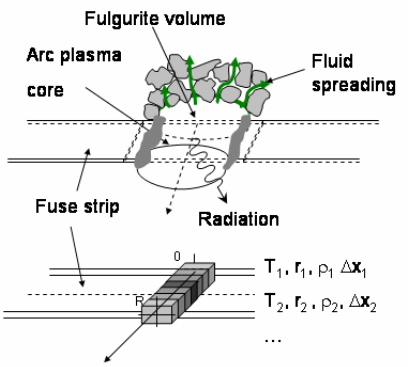

Fig. 4: Schematic explanation of the geometry chosen for the calculation ; $x = 0$ corresponds to the edge of the fuse strip in the sand, $x = R$ corresponds to the edge in contact with the quartz window from which the light is integrated.

Figure 4 illustrates the fulgurite and the plasma volume in the case of the experimental fuse. The back edge of the fulgurite is delimited by the silica sand grains, and the front edge of the plasma volume is in contact with the quartz window from which the light is collected. The calculation is performed for the domain $x \in [0,R]$ and it is assumed that the radiation is emitted in the R-direction only, in so far as in the 0-direction the radiation is unable to escape.

978-2-84516-363-8/07/$25.00 © 2007
Blaise Pascal Academic Press

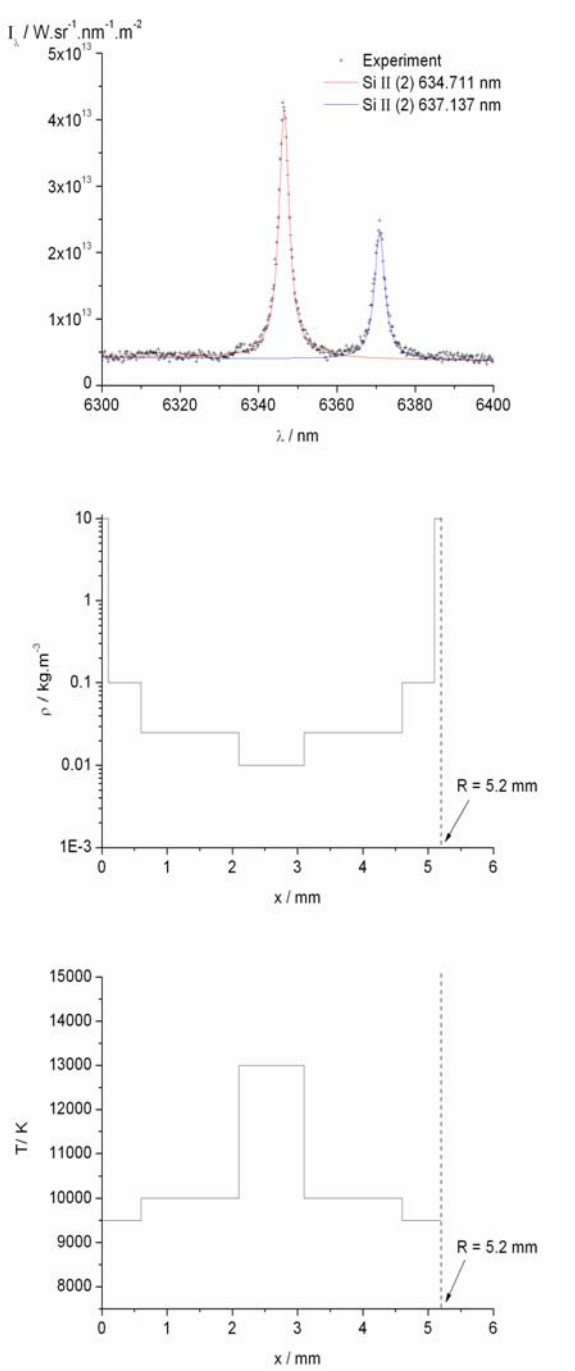

Fig. 5: Comparison at $t_4 = 3.24$ ms between experiment and calculation for the Si II (2) multiplet: spectral profile, plasma density, and temperature. $T_{EXP} = 11{,}988$ K.

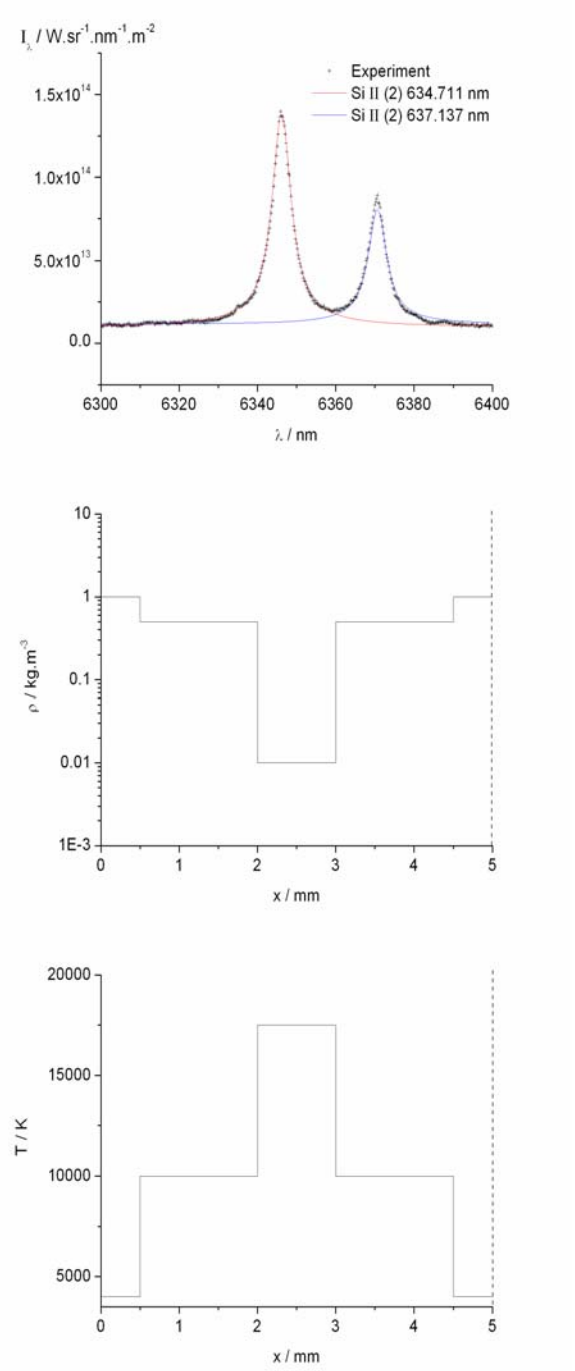

Fig. 6: Comparison at $t_3 = 2.97$ ms between experiment and calculation for the Si II (2) multiplet: spectral profile, plasma density, and temperature. $T_{EXP} = 12{,}914$ K.

In the lower part of Fig. 4 we show the configuration chosen for the calculation. We consider that the experimental observation corresponds to one line of sight which is divided in a fixed number of volume elements of length Δx_k from $x = 0$ to $x = R$ ($k = 1,2,\ldots$).

For each Δx_k : the temperature value is fixed according to the mean temperature obtained for the same observation time by spectroscopic diagnostic, and the plasma density value is set according to the experimental electron density. The variations of the temperature and the plasma density are chosen symmetrical to the axis of symmetry of the fuse

978-2-84516-363-8/07/$25.00 © 2007
Blaise Pascal Academic Press

strip. The calculation is done for $t_1 = 2.43$ ms, $t_2 = 2.70$ ms, $t_3 = 2.97$ ms, $t_4 = 3.24$ ms (Fig. 2). The first result is given in Fig. 5 for $t_4 = 3.24$ ms, that is to say during the decrease of the electric power near the end of the arcing time.

The characteristics of the domain are given for the temperature and the plasma density. For these values we see that the calculated profiles fit well with the experimental profile. The plasma density decreases strongly from 10 kg.m^{-3} at $x = 0$ down to 0.01 kg.m^{-3} in the centre.

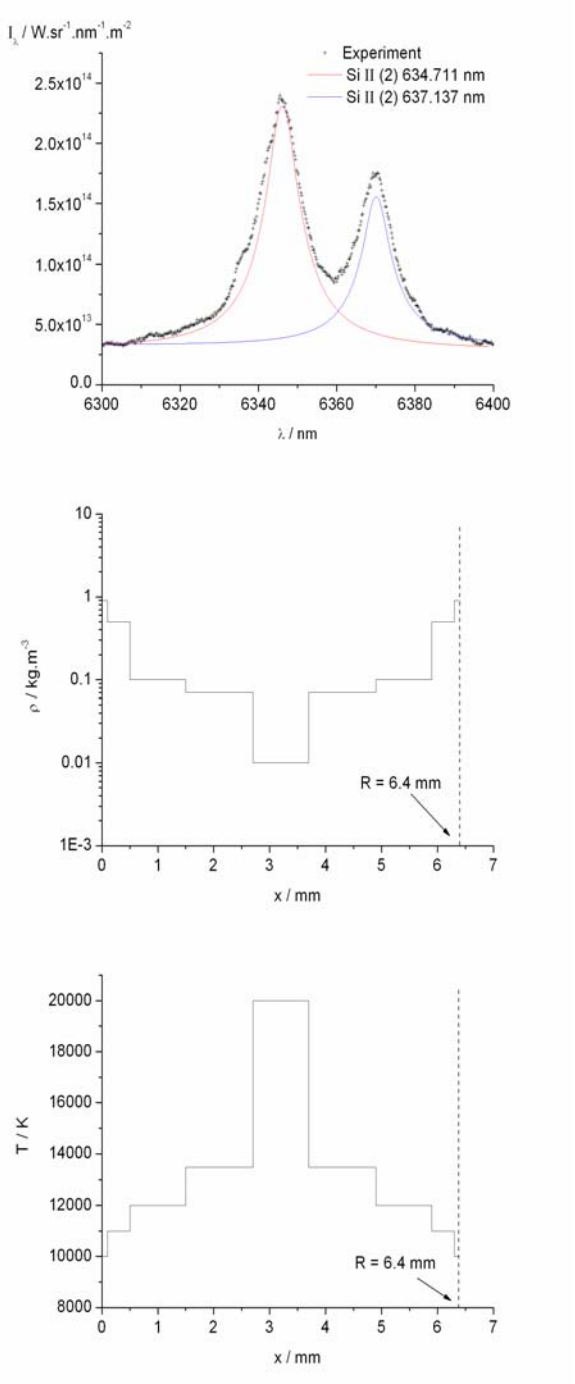

Fig. 7: Comparison at $t_2 = 2.70$ ms between experiment and calculation for the Si II (2) multiplet: spectral profile, plasma density, and temperature. T_{EXP} = 13,839 K.

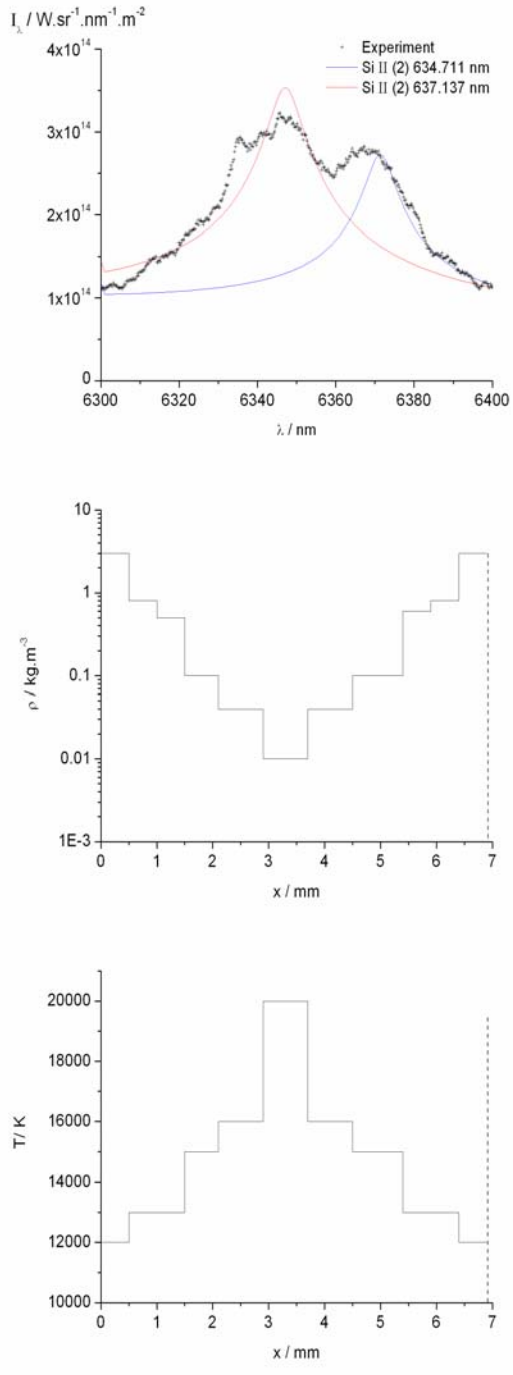

Fig. 8: Comparison at $t_1 = 2.43$ ms between experiment and calculation for the Si II (2) multiplet: spectral profile, plasma density, and temperature. T_{EXP} = 14,765 K.

978-2-84516-363-8/07/$25.00 © 2007
Blaise Pascal Academic Press

The plasma temperature increase from 9500 K at $x = 0$ to 13000K in the centre. The calculated trend for the temperature clearly shows that the experimental temperature can not be considered as uniform on the whole plasma thickness.

On the contrary the experimental temperature has to be considered as a mean value of the temperature which is the result of the contribution of different volumes with a given temperature.

Similar results are obtained for t_3 and t_2. We can notice that there is an increase of the domain $[0, R]$ with higher values of R. This is consistent with the fact that for this time interval the pressure increases – linked to the increase of the temperature, and the vaporization – and implies a higher width of the plasma volume. For the spectral observations given on Fig. 5 to Fig. 8, the width of the two reduced sections fuse element is 5 mm in the initial state. The corresponding widths put in the calculation are 5.2 mm, 5 mm, 6.4 mm and 6.9 mm respectively for t_4, t_3, t_2 and t_1. This parameter is difficult to determine in so far as the fuse arc plasma radiation is collected through a quartz window directly in contact with the plasma. Thus the plasma interacts with the quartz window and can imply strong fluctuations at the surroundings.
Moreover the experimental temperature increases regularly from t_4 to t_1. This trend is consistent with the increase of the calculated maximum temperature observed close to $x = R/2$. For t_4, t_3, t_2 and t_1 we obtain respectively 13,000 K, 17,500 K, and 20,000 K for t_2 and t_1. These values can not be considered as the true values but the rise seems to be in good agreement with the rise in pressure and electron density.

The case $t_1 = 2.43$ ms is more problematic because it corresponds to a high level of electric power: the continuous radiation is strong and the spectral lines are strongly broadened. From Fig. 2 and Fig. 3c we see that this time is close to the time for which it is difficult to distinguish the discret radiation from the continuous radiation. The calculation has been tested to evaluate if it is able to give a realistic result concerning the influence of the plasma density and temperature, especially to estimate the conditions implying a strong broadening with a dissymmetrical spectral line shape like in experiments. The result of the calculation is given in Fig. 8 for $t_1 = 2.43$ ms. The experimental profiles are strongly disturbed and the calculated profiles do not fit well with the experimental ones.

This case illustrates clearly the limit of the calculation. From our opinion the time domain corresponding to the time observation with $t < t_1$ is characterized by very strong and quick variations of the gradients in temperature, pressure, plasma density, plasma composition and also in the dependant properties such as the optical thickness of the plasma. Such observations have been made in the case of the interaction between a metallic plasma and a polymer wall [39]. In this latter case the rise in pressure is highly brisk and the pressure value is high. It implies the spreading of the pressure wave with transmitted and reflected components. The interference between these two components is directly linked to the strong broadening of the spectral lines, to the increase of the continuous radiation intensity, and to the strong increase of the plasma optical thickness that implies absorption of the emitted radiation. In this case also the spectral line shape can not be used for a spectroscopic diagnostic and other experimental methods have to be used.

4. Synthesis and conclusion

For modelling purposes [40] one has to calculate the radiative term of the fuse arc plasma. This calculation consists in the evaluation of the evolution of the net emission coefficient versus the temperature for a given plasma composition. But the hypotheses linked to the calculation have to be checked. The way described in this study is to compare the experimental spectrum observed during the fuse operation with the result of the calculation including the continuous and spectral components.

The first attempt given in this paper clearly shows that some hypotheses have to be used with great care, especially:

• the calculation of the radiation is usually a complex task, and especially in the case of the fuse working as far as the plasma volume is not a cylindrical volume well appropriate to use classical methods such as the Abel inversion necessary to obtain the local emissivities ;

• due to the short duration of the arcing time – typically around 5 ms – there exist strong gradients which evolve on the whole duration of the fuse working ; these gradients concern the temperature, the plasma composition, the optical thickness, the values of the transport coefficients, namely the electrical conductivity, the thermal conductivity, and the viscosity ;

• therefore the following assumptions have to be discussed:

- *the plasma is supposed in Local Thermodynamic Equilibrium (LTE)*: this can be easily justified for the areas close to the centre of the fuse arc plasma because the pressure is high ; but for the areas close to the surroundings, near the fused silica layer surrounding the plasma core, and near

978-2-84516-363-8/07/$25.00 © 2007
Blaise Pascal Academic Press

the quartz window, the gradients are very high and the LTE hypothesis is not valid ; these areas correspond to the colder surroundings ;

- *the influence of the spectroscopic constants* : in the case of the radiation measurements by means of spectroscopy, and the calculation of the discret and continuous radiations, one uses the transition strengths A_{ul} quoted in various databases ; if possible, the experimental values are preferred but usually these experimental values correspond to measurements performed in different plasma sources ; and most of these plasma sources are uniform in temperature, density and the influence of the gradients in physical properties is negligible ; in the case of the fuse arc plasma, the pressure is very high and can affect the transition strengths;
- *the variations of the plasma composition* : the composition of the plasma at a given time of observation is one of the key parameters to obtain a consistent assessment of the radiation ; as it has been shown in [37] an addition of metallic species implies very strong changes in the resulting plasma composition for a given temperature ; thus the radiated intensity is modified and it depends directly on the concentration of these metallic species ; furthermore the radiated properties of the metallic spectral lines is hard to calculate as soon as the pressure moves far away the atmospheric pressure: the low energy level of two typical silver lines, namely Ag I 520,907 nm and Ag I 546.550 nm, is close to the ground level of the silver atom ; therefore these lines are highly subjected to self-absorption when they are observed during the fuse working ; such lines are unusable for a spectroscopic diagnostic, and the calculation of the emissivity should imply a specific knowledge of the physical characteristics of the fuse arc plasma.
- *the influence of the calibration of the experimental observation* : due to the geometry of the experimental fuse, it is rather complex to perform a valuable calibration in intensity ; many mistakes can be made and they make more difficult the choice of the initial values in the calculation.

The comparison of the experimental and theoretical intensities given in this paper clearly shows a good agreement at the end of the arcing time. The calculation of the discrete and the continuous radiations fits well with the measurement. The calculated broadening and shifting of the Si II (2) lines by Stark effect are also in good agreement. But for the time corresponding to high levels of electric power and pressure, the calculation of the continuum in particular becomes more complicated as far as it depends strongly on the concentration of the various chemical species in the fuse arc plasma.

The next step of this work is thus to improve the depiction of the $x \in [0, R]$ domain. Physical arguments have to be defined in order to build an iterative calculation for the determination of Δx_k . A solution could be to calculate the radiation for the final microseconds of radiation emission for the lowest levels of the electric power. By means of the high sensitivity CCD matrix the radiation emission can be observed even if the level of radiation is very low. In this case the broadening of the spectral is minimum and the contribution of the Stark broadening is very weak in the total broadening. The main broadening is due to the apparatus function.

In the future these calculations could be very helpful to define the true net emission coefficients used in the modelling of the fuse working.

Acknowledgements

First, we thank both for their financial support and their help through many discussions, Mr. J.L. Gelet and Mr. T. Rambaud from Ferraz Shawmut, Mr. J.C. Perez Quesada from Mesa, and Mr. F. Gentils from Schneider Electric.

Second, we thank Dr. D. Hofsaess for having provided the ξ_{bf} and ξ_{ff} factors to calculate the continuum.

References

[1] T Chikata, Y Ueda, Y Murai, T Miyamoto, Spectroscopic observations of arcs in current limiting fuse through sand, Proceedings of the Icefa (Liverpool, England), April, pp 114-121, 1976

[2] P. Bezborodko, J. Fauconneau, R. Pellet, Experimental set-up for spectroscopic measurements of plasma arcs in fuses, Proceedings of the 5th Icefa (TU Ilmenau, Germany), 25-27 Sept., pp 259-264, 1995

[3] W. Bussière, P. Bezborodko, R. Pellet, Spectroscopic study of a cutting electrical arc in HBC fuse, Proceedings of the 6th Icefa (IEN Galileo Ferraris, Torino, Italy), 20-22 Sept., pp 113-118, 1999

[4] M.A. Saqib, A.D. Stokes, B.W. James, I.S. Falconner, Arc temperature measurement in a high voltage fuse, Proceedings of the 6th Icefa (IEN Galileo Ferraris, Torino, Italy), 20-22 Sept., pp 107-112, 1999

[5] L. Cheim, A. Howe, Spectroscopic measurement of fuse arc temperature, Proceedings of the 5th Icefa (TU Ilmenau, Germany), 25-27 Sept., pp 251-258, 1995

[6] L. Cheim, Arc temperature measurements in high breaking capacity fuses, PhD. Thesis, Univ. of Nottingham, Dpt. of Electrical & Electronic Engineering, December, 1992

[7] M.A. Saqib, A.D. Stokes, B.W. James, I.S. Falconner, Measurement of electron density in a high voltage fuse arc, Proceedings of the 6th Icefa (IEN Galileo Ferraris, Torino, Italy), 20-22 Sept., pp 107-112, 1999

978-2-84516-363-8/07/$25.00 © 2007
Blaise Pascal Academic Press

[8] W. Bussière, Mesure des grandeurs (T,Ne,P) au sein du plasma d'arc des fusibles en moyenne tension, PhD. Thesis (in French), Univ. Blaise Pascal, D.U. 1258, December, 2000
[9] W. Bussière, Influence of sand granulometry on electrical characteristics, temperature and electron density during high-voltage fuse arc, J.Phys.D:Appl. Phys. 34, pp 925-935, 2001
[10] Lakshiminarashima C S, Barrault M R and Oliver R, Factors influencing the formation and structure of fuse fulgurites, IEE Proc., Sci. Meas. Technol., 125, 391–399, 1978
[11] Wilkins R, Gnanalingam S, Burn-back rates of silver, fuse elements, 5th Int. Conf. on Gas Discharges (University of Liverpool), 195–198, 1978
[12] W. Bussière, Estimation of the burn-back rate in high breaking capacity fuses using fast imagery, J.Phys.D:Appl. Phys. 34, 1-10, 2001
[13] M.A. Saqib, A.D. Stokes, P.J. Seebacher, Pressure inside the arc channel of a high-voltage fuse, Proceedings of the 6th Icefa (IEN Galileo Ferraris, Torino, Italy), 20-22 Sept., pp 83-88, 1999
[14] D. Rochette, W. Bussière, Pressure evolution during HBC fuse operation, Plasma Sources Sci. and Technol., 13, pp 293-302, 2004.
[15] W. Bussière, P. André, Evaluation of the composition, the pressure, the thermodynamic properties and the monoatomic spectral lines at fixed volume for a SiO2_Ag plasma in the temperature range 5000-25000 K, J.Phys.D: Appl. Phys. 34, pp 1665-1674, 2001
[16] O. Bouilliez, J.C. Perez-Quesada, Conception et utilisation de fusibles limiteurs MT, Cahier Technique n°128, Ed. Schneider Electric, Collection Technique, Novembre 2002.
[17] A. Lesage, R.A. Rathore, I.S. Lakicevic, J. Puric, Stark widths and shifts of singly ionized silicon spectral lines, Phys. Rev. A. 28, pp 2264-2268, 1983
[18] NIST Atomic Spectra Database Lines Form, http://physics.nist.gov/PhysRefData/ASD/lines_form.html
[19] J. Menart, J. Herbelein, E. Pfender, Line-by-line method of calculating emission coefficients for thermal plasmas consisting of monatomic species, J. Quant. Spectrosc. Radiat. Transfer, Vol. 56, N°3, pp 377-398, 1996
[20] F. Cabannes, J. Chapelle, Reactions under plasmas conditions, Chap. VII, Spectroscopic plasma diagnostic, Ed. M. Venugopalan (Wiley Interscience, NY), Vol. 1, 367-469, 1971
[21] E.E. Whiting, An empirical approximation to the Voigt profile, J. Quant. Spectrosc. Radiat. Transfer, Vol. 56, N°3, pp 377-398, 1996
[22] G. Traving, Plasma Diagnostics, Ed. by W. Lochte-Holtgreven, Wiley NY, 66-134, 1968
[23] J. Richter, Plasma Diagnostics, Ed. by W. Lochte-Holtgreven, Wiley NY, 1-65, 1968
[24] H.R. Griem, Spectral Line Broadening by Plasmas, Academic Press, NY, 1974
[25] H.R. Griem, Principles of Plasma Spectroscopy, Cambridge University Press, 1997
[26] L.G. D'yachkov, The calculation of continuous radiative spectra, Translated from Teplofizika Vysokikh Temperatur, Vol. 30, N°5, 868-875, Sept-Oct, 1992
[27] M.I. Boulos, P. Fauchais, E. Pfender, Thermal plasmas – Fundamentals and applications, Vol. 1, Ed. Plenum Press (N.Y. and London), 1994
[28] S.E. Schnehage, M. Kock, E. Schulz-Gulde, The continuous emission of an argon arc, J. Phys. B: At. Mol. Phys., 15, 1131-1135, 1982
[29] H. Kafrouni, S. Vacquie, Study of the recombination continuum in an SF6 arc discharge, J. Quant. Spectrosc. Radiat. Transfer, Vol. 32, N°3, 219-224, 1984
[30] D. Hofsaess, Emission continua of rare gas plasmas, J. Quant. Spectrosc. Radiat. Transfer, Vol. 19, 339-352, 1978
[31] L.G. D'yachkov, G.A. Kobzev, P.M. Pankratov, Continuous radiation of a dense plasma on inert gases: analysis of experimental data, High Temperature, Vol. 34, N°6, 855-863, 1996
[32] Y. Vitel, L.G. D'yachkov, Yu K. Kurilenkov, Radiation continuum of dense krypton plasma, J. Phys. B: At. Mol. Phys., 30, 2021-2031, 1997.
[33] A Gleizes, J J Gonzalez, P Freton, Thermal plasma modelling, J. Phys. D: Appl. Phys., 38, N°9, R153-R183, 2005
[34] A Gleizes, J J Gonzalez, B Liani, G Raynal, Calculation of net emission coefficient of thermal plasmas in mixtures of gas with metallic vapour, J. Phys. D: Appl. Phys., 26, N°11, 1921-1927, 1993
[35] D. Hofsaess, Photoionization cross sections calculated by the scaled Thomas-Fermi method, Atomic Data and Nuclear Date Tables, 24, 285-321, 1979
[36] D. H. Menzel, C.L. Pekeris, Monthly Notices of the Royal Astronomy Society, 96, 77-?, 1935
[37] P. André, W. Bussière, D. Rochette, Transport coefficients of Ag-SiO2 plasmas, Plasma Chemistry and Plasma Processing, To be published, DOI. 10.1007/s11090-007-9086-y
[38] D. Rochette, W. Bussière, P. André, Composition, enthalpy and vaporization temperature calculation of Ag-SiO_2 plasmas with air in the temperature range from 1000 to 6000 K and for pressure included between 1 to 50 bars, Plasma Chemistry and Plasma Processing, Vol. 24, N°3, 475-491, 2004
[39] W. Bussière, E. Duffour, P. André, R. Pellet, L. Brunet, Experimental assessment of temperature in plasma wall interaction. Application to PE and POM., Eur. Phys. J. D 28, 79–90, 2004
[40] D. Rochette, S. Clain, W. Bussière, Mathematical model using macroscopic and microscopic scales of an electrical arc discharge through a porous medium in HBC fuses, Proceedings of the 7th Icefa (Gdansk Univ. of Tech., Gdansk, Poland), 8-10 Sept., pp 188-193, 2003

978-2-84516-363-8/07/$25.00 © 2007
Blaise Pascal Academic Press